Comparative proteomic analysis identifies exosomal Eps8 protein as a potential metastatic biomarker for pancreatic cancer

KEIICHI OHSHIMA[1], KEIICHI HATAKEYAMA[1], KAORI KANTO[1], TOMOMI IDE[1], YUKO WATANABE[1], SACHI MOROMIZATO[1], KANAKO WAKABAYASHI-NAKAO[1,3], NAOKI SAKURA[1], KEN YAMAGUCHI[2] and TOHRU MOCHIZUKI[1]

[1]Medical Genetics Division, Shizuoka Cancer Center Research Institute;
[2]Shizuoka Cancer Center Hospital and Research Institute, Shizuoka 411-8777, Japan

Received June 12, 2018; Accepted November 1, 2018

DOI: 10.3892/or.2018.6869

Abstract. Exosomes are small vesicles found in extracellular environments including blood, urine, and cell culture medium. Their contents are cell-type specific, and molecules embedded in exosomes can be useful fluid-based clinical biomarkers. To identify proteins with metastatic marker potential, we conducted a comparative exosomal proteome analysis using human pancreatic cancer cell lines derived from metastasis, ascites, and primary tumors. Metastatic potential of cell lines was assessed by migratory and invasive activities. A pancreatic cancer cell line from metastasis (SU.86.86) revealed 23-fold and 20-fold increases in cell migratory and invasive activities, respectively, compared to the MIA PaCa-2 cell line derived from primary tumor cells. Liquid chromatography-mass spectrometry-based proteome analysis and subsequent validation by immunoblot analysis revealed that epidermal growth factor receptor pathway substrate 8 (Eps8) was highly abundant in exosomes from metastasis-derived SU.86.86 cells. Comparison of 12 pancreatic cancer cell lines derived from different stages of malignancy revealed a strong relationship between exosomal Eps8 protein levels and cell motile activities (migration: r=0.85, P=4.2x10-4; invasion: r=0.60, P=3.2x10-2). Conversely, relationships between intracellular Eps8 protein levels and cell motile activities were moderate (migration: r=0.65, P=2.0x10-2; invasion: r=0.51, P=9.2x10-2). It was therefore concluded that exosomal Eps8 protein levels were correlated with the migratory cell potential of human pancreatic cancer cells, indicating that exosomal Eps8 has the potential to be a metastatic biomarker for human pancreatic cancer.

Correspondence to: Dr Keiichi Ohshima, Medical Genetics Division, Shizuoka Cancer Center Research Institute, 1007 Shimonagakubo, Nagaizumi-Cho, Sunto-Gun, Shizuoka 411-8777, Japan
E-mail: k.ohshima@scchr.jp

[3]*Present address:* Department of Pharmaceutical Sciences, International University of Health and Welfare, 2600-1 Kitakanemaru, Otawara, Tochigi 324-8501, Japan

Abbreviations: CM, culture medium; Ct, cycle threshold; EGF, epidermal growth factor; Eps8, epidermal growth factor receptor pathway substrate 8; FBS, fetal bovine serum; GAPDH, glyceraldehyde 3-phosphate dehydrogenase; LC-MS/MS, liquid chromatography-mass spectrometry; RTCA, real-time cell analysis; SDS-PAGE, SDS-polyacrylamide gel electrophoresis

Key words: Eps8, exosomes, pancreatic cancer, metastasis, pancreatic cancer cell line, proteomics, biomarker

Introduction

Exosomes are 30-100 nm membranous organelles that are released from cells into the extracellular microenvironment (1). Exosomes are vesicular carriers for intercellular communication, and they contain various signaling biomolecules, including proteins, metabolites, RNA, DNA, and lipids to target cells (2-4). Mass spectrometry and microarray technologies have been used to perform exosomal biomolecules profiling. These efforts have revealed that exosomal biomolecule composition varies depending on the cell type of origin (1,5). Since exosomes are found in biological fluids, including blood and urine, exosomal biomolecules with disease specificity are promising targets in liquid biopsies (6).

Cancer diagnosis at an early stage, before it has grown and spread to other organs by metastasis, is a prerequisite for successful treatment. Pancreatic cancer is one of the most deadly cancer forms and the third leading cause of cancer-related deaths in the United States (7), the EU (8) and Japan (http://ganjoho.jp/en/professional/statistics/brochure/2017_en.html). Early stage pancreatic cancer is difficult to diagnose since it is asymptomatic, making pancreatic cancer particularly challenging to treat and/or cure (9). In most cases, pancreatic cancer growth and metastasis have occurred by the time of diagnosis, leading to the poorest outcomes among the major types of cancer with a 5-year survival rate of <10% (7). While early diagnosis is essential for effective pancreatic cancer treatment and/or cure, there are currently no proven clinical tumor markers for the early stages of pancreatic cancer. However, recent developments in molecular profiling technologies have indicated that proteins and microRNAs identified in exosomes could be useful as fluid-based diagnostic and prognostic markers for pancreatic cancer (10,11).

Cell culture systems have been used for secretome analyses to identify the extracellular or exosomal proteins and microRNAs released into the medium (12-14). Using cancer cells coupled with proteomics- or transcriptomics-based approaches, we have identified an abundance of polyadenylate binding protein 1 and let-7 family microRNAs in exosomes isolated from metastatic duodenal cancer cells (15,16). In the present study, we aimed to identify pancreatic cancer metastasis. We performed exosomal proteome analysis using pancreatic cancer cell lines derived from early (primary tumors), and late stages (ascites, and metastatic tumors) of tumor progression. Comparative analyses revealed that epidermal growth factor receptor pathway substrate 8 (Eps8) protein was abundant in exosomes derived from metastatic tumors and ascites and that the amount of exosomal Eps8 was quantitatively correlated with the *in vitro* cell migratory activity. These observations indicating that exosomal Eps8 is a predictive biomarker for pancreatic cancer metastasis.

Materials and methods

Cell culture. Cell lines used in the present study are listed in Table I. Cells were maintained in a humidified atmosphere (37˚C, 5% CO_2) in RPMI-1640 medium (Sigma-Aldrich; Merck KGaA, Darmstadt, Germany) supplemented with 2 mM L-glutamine (Nissui Pharmaceutical, Co., Ltd., Tokyo, Japan), 100 U/ml penicillin-100 mg/ml streptomycin, and 10% heat-inactivated (FBS) (all from Thermo Fisher Scientific, Inc., Waltham, MA, USA).

Cell migration and invasion assays. Real-time cell analysis (RTCA) of *in vitro* cell migratory and invasive activities was performed using an xCELLigence RTCA DP instrument (Roche Diagnostics, Indianapolis, IN, USA) as previously described (15). Samples were analyzed in quadruplicate as technical replicates. Data analysis was performed using the RTCA software (version 1.2) supplied with the instrument.

Production and isolation of exosomes. Exosomes were isolated from the cell culture medium as previously described (15,16). Briefly, cells were cultured for 48 h at 37˚C with 5% CO_2 in complete RPMI-1640 medium containing 10% FBS depleted of contaminating microvesicles by centrifugation at 100,000 x g for 18 h. Culture medium (CM) was collected and centrifuged at 800 x g for 5 min and at an additional 2,000 x g for 10 min to remove detached cells. The supernatant was then filtered through a 0.1-μm pore polyethersulfone membrane filter (Thermo Fisher Scientific, Inc.) to remove cell debris and large vesicles, then concentrated using a Centricon Plus-70 with a 100,000-MW cut-off membrane (EMD Millipore; Billerica, MA, USA). Concentrated CM was ultracentrifuged at 100,000 x g for 2 h at 4˚C using a 70Ti rotor (Beckman Coulter, Inc., Brea, CA, USA). Resultant pellets were resuspended in 6 ml phosphate-buffered saline (PBS) and ultracentrifuged at 100,000 x g for 1 h at 4˚C using a 100Ti rotor (Beckman Coulter, Inc.).

Proteome analysis using mass spectrometry. Exosomal proteome analysis was performed by LC-MS/MS (liquid chromatography-mass spectrometry) as previously described (15,17). Proteins (200 μg) from isolated exosomes were dissolved in lysis buffer containing 7.5 M urea and 2.5 M thiourea (both from Sigma-Aldrich; Merck KGaA), 12.5% glycerol (Chemical Industries, Osaka, Japan), 50 mM Tris, 2.5% n-octyl-β-D-glucoside, 6.25 mM Tris(2-carboxyethyl) phosphine hydrochloride, and 1.25 mM protease inhibitor (all from Sigma-Aldrich; Merck KGaA) before being rotated at 4˚C for 60 min. After centrifugation at 14,000 x g for 60 min at 4˚C, the supernatant was fractionated using the Agilent 1200 HPLC system (Agilent Technologies, Inc., Santa Clara, CA, USA) with an Intrada WP-RP column (0.46x25 cm, 3-μm particle size and 30-nm pore size; Imtakt, Kyoto, Japan). Collected fractions were digested with trypsin (Promega Corp., Madison, WI, USA) and analyzed by LC-MS/MS using a nanoflow LC-ESI linear ion trap-TOF NanoFrontier L mass spectrometer (Hitachi High-Technologies, Tokyo, Japan). Raw LC-ESI data were converted to peak list files using NanoFrontier L Data Processing software (Hitachi High-Technologies). The peak list files were used for protein identification with the MASCOT MS/MS ion search (http://www.matrixscience.com) and X! Tandem software (http://www.thegpm.org). Upon peptide sequence annotation, the UniProtKB/Swiss-Prot database (version 2016_10; *Homo sapiens*; http://www.uniprot.org/statistics/Swiss-Prot) was used with the following parameters: enzyme, trypsin or none (when used with the home-made dataset only); maximum number of missed cleavage, 1; peptide tolerance, 0.2 Da; MS/MS tolerance, 0.2 Da; variable modification, oxidation of methionine; and peptide charge, (1+, 2+ and 3+). All identified proteins with MASCOT threshold scores < 95% confidence level and peptide numbers <2 were then removed from the protein list using Scaffold software (http://www.proteomesoftware.com/products/scaffold/).

Immunoblot analysis. Exosomes and cells were lysed with 7.5 M urea-based lysis buffer as described above. Protein concentrations were determined by the Bradford assay (Bio-Rad Laboratories, Inc., Hercules, CA, USA). Proteins (5 or 10 μg) were subjected to 8% SDS-polyacrylamide gel electrophoresis (SDS-PAGE), and transferred onto an Immobilon-P polyvinylidene fluoride (*PVDF*) membrane (0.45-mm pore size; EMD Millipore). PVDF membranes were blocked for 1 h at room temperature in Tris-buffered saline (10 mM Tris-HCl, pH 7.5, 150 mM NaCl) containing 0.01% Tween-20 and 5% non-fat dried milk (Wako Pure Chemical Industries). Blocked membranes were then incubated overnight at 4˚C with primary monoclonal antibodies (listed in Table II). Membranes were then incubated for 1 h at room temperature with anti-mouse IgG antibodies conjugated with horseradish peroxidase (Table II). Specific proteins were visualized using an ECL Plus western blotting detection system (GE Healthcare, Wauwatosa, WI, USA) and a Fujifilm Luminescent Image Analyzer LAS3000 (Fujifilm, Tokyo, Japan). The molecular weight of each protein was deduced using Precision Plus Protein All Blue Standards (Bio-Rad Laboratories, Inc.).

RNA isolation and quantitative RT-PCR analysis. Cells were cultured for 48 h, and total RNA was extracted using the miRNeasy Mini Kit (Qiagen, Hilden, Germany) as previously described (15). RNA samples were quantified with a NanoDrop spectrophotometer (Thermo Fisher Scientific, Inc.) and

Table I. List of human cancer cell lines used in the present study.

Tissue	Cell line	Histology	Supplier	Catalogue no.	Derivation
Pancreas	SU.86.86	Ductal carcinoma	ATCC[a]	CRL-1837	Liver metastasis
	CFPAC-1	Ductal adenocarcinoma	ATCC	CRL-1918	Liver metastasis
	KP-3	Adenosquamous carcinoma	JCRB[b]	JCRB0178.0	Liver metastasis
	PK-45H	Carcinoma	RCB[c]	RCB1973	Liver metastasis, derived from the same patient as PK-45P
	PK-1	Carcinoma	RCB	RCB1972	Liver metastasis, derived from the same patient as KLM-1
	PK-8	Carcinoma	RCB	RCB2700	Liver metastasis
	PK-59	Carcinoma	RCB	RCB1901	Liver metastasis
	KLM-1	Carcinoma	RCB	RCB2138	Liver metastasis, derived from the same patient as PK-1
	SW 1990	Adenocarcinoma	ATCC	CRL-2172	Spleen metastasis
	Hs 766T	Carcinoma	ATCC	HTB-134	Lymph node metastasis
	Capan-1	Adenocarcinoma	ATCC	HTB-79	Liver metastasis
	HuP-T3	Adenocarcinoma	ECACC[d]	93121055	Ascites
	HuP-T4	Adenocarcinoma	ECACC	93121056	Ascites
	HPAFII	Adenocarcinoma	ATCC	CRL-1997	Ascites
	AsPC-1	Adenocarcinoma	ATCC	CRL-1682	Ascites
	MIA PaCa-2	Carcinoma	ATCC	CRL-1420	Primary tumor
	BxPC-3	Adenocarcinoma	ATCC	CRL-1687	Primary tumor
	PK-45P	Carcinoma	RCB	RCB2141	Primary tumor, derived from the same patient as PK-45H
	Capan-2	Adenocarcinoma	ATCC	HTB-80	Primary tumor
	PSN1	Adenocarcinoma	ECACC	94060601	Primary tumor
	PANC-1	Epithelioid carcinoma	ATCC	CRL-1469	Primary tumor
	Panc 10.05	Adenocarcinoma	ATCC	CRL-2547	Primary tumor
Stomach	KATOIII	Signet ring cell carcinoma	JCRB	JCRB0611	Pleural effusion and lymph node metastasis
	SNU-1	Carcinoma	ATCC	CRL-5971	Primary tumor
	SNU-16	Carcinoma	ATCC	CRL-5974	Ascites
	NUGC-3	Adenocarcinoma, poorly differentiated	JCRB	JCRB0822	Brachial muscle metastasis
	NUGC-4	Adenocarcinoma, poorly differentiated, signet ring cell carcinoma	JCRB	JCRB0834	Lymph node metastasis
	MKN45	Adenocarcinoma, poorly differentiated	JCRB	JCRB0254	Primary tumor
	MKN45P	Subcloned from MKN45[38]			Peritoneal metastasis in mice inoculated with MKN45
Duodenum	AZ-521	Carcinoma	JCRB	JCRB0061	Primary tumor, identical genotype to HuTu 80 revealed by short Tandem repeat analysis
	AZ-P7a	Subcloned from AZ-521[39]			Peritoneal metastasis in mice inoculated with MKN45

Table I. Continued.

Tissue	Cell line	Histology	Supplier	Catalogue no.	Derivation
Colon	COLO 201	Dukes' type D, colorectal adenocarcinoma	JCRB	JCRB0226	Ascites, derived from the same patient as COLO 205
	COLO 205	Dukes' type D, colorectal adenocarcinoma	ATCC	CCL-222	Ascites, derived from the same patient as COLO 201
	LoVo	Dukes' type C, grade IV, colorectal adenocarcinoma	ATCC	CCL-229	Left supraclavicular region metastasis
	DLD-1	Dukes' type C, colorectal adenocarcinoma	ECACC	90102540	Primary tumor
	HT115	Carcinoma	ECACC	85061104	Primary tumor
Lung	PC-10	Squamous cell carcinoma	IBL[e]	IBL37013	Primary tumor
	LK-2	Squamous cell carcinoma	JCRB	JCRB0829	Primary tumor
	EBC-1	Squamous cell carcinoma	JCRB	JCRB0820	Skin metastasis
	NCI-H520	Squamous cell carcinoma	ATCC	HTB-182	Primary tumor
	SBC-1	Small cell carcinoma	JCRB	JCRB0816	Primary tumor
	SBC-3	Small cell carcinoma	JCRB	JCRB0818	Bone marrow metastasis
	NCI-H1581	Large cell carcinoma	ATCC	CRL-5878	Primary tumor
	NCI-H1650	Adenocarcinoma	ATCC	CRL-5883	Pleural effusion metastasis
	COR-L23	Large cell carcinoma	ECACC	92031919	Pleural effusion metastasis
Thyroid	TT	Medullary carcinoma	ATCC	CRL-1803	Primary tumor
	K1	Papillary thyroid carcinoma	ECACC	92030501	Primary tumor
	8505C	Undifferentiated thyroid carcinoma	JCRB	JCRB0826	Primary tumor
Esophagus	KYSE30	Squamous cell carcinoma	JCRB	JCRB0188	Primary tumor
	KYSE220	Squamous cell carcinoma	JCRB	JCRB1086	Primary tumor
EGJ	OE19	Adenocarcinoma	ECACC	96071721	Primary tumor
Prostate	LNCaP	Carcinoma	ATCC	CRL-1740	Lymph node metastasis
	DU145	Carcinoma	ATCC	HTB-81	Brain metastasis
	PC-3	Grade IV, adenocarcinoma	ATCC	CRL-1435	Bone metastasis
Breast	Hs 578T	Carcinoma	ECACC	86082104	Primary tumor
	SK-BR-3	Adenocarcinoma	ATCC	HTB-30	Pleural effusion metastasis
	T-47D	Ductal carcinoma	ATCC	HTB-133	Pleural effusion metastasis
Urinary bladder	5637	Grade II carcinoma	ATCC	HTB-9	Primary tumor
	T24	Transitional cell carcinoma	ATCC	HTB-4	Primary tumor
	SCaBER	Squamous cell carcinoma	ATCC	HTB-3	Primary tumor
Liver	SK-HEP-1	Adenocarcinoma	ECACC	91091816	Ascites
	Hep G2	Hepatoblastoma[40]	ATCC	HB-8065	Primary tumor

[a]American Type Culture Collection (Manassas, VA, USA); [b]Japanese Collection of Research Bioresources (Osaka, Japan); [c]RIKEN BioResourse Center (Ibaraki, Japan); [d]European Collection of Cell Cultures (Salisbury, UK), [e]Immuno-Biological Laboratories (Gunma, Japan). EGJ, esophagogastric junction.

Table II. List of antibodies used for western blot analysis.

Protein	Clonality	Host	Supplier	Catalogue no.	Dilution	Dilution of 2nd Ab
Eps8	Monoclonal	Mouse	BD Biosciences[a]	610144	1:5,000	1:10,000[d]
α-tubulin	Monoclonal	Mouse	EMD Millipore[b]	CP06	1:5,000	1:10,000[d]
GAPDH	Monoclonal	Mouse	SCBT[c]	sc-36562	1:1,000	1:5,000[d]

[a]BD Biosciences, San Jose, CA, USA; [b]EMD Millipore, Billerica, MA, USA; [c]Santa Cruz Biotechnology, Inc., Dallas, Texas, USA; dSecondary antibody conjugated with horseradish peroxidase: Goat anti-mouse IgG antibody (cat. no. 115-035-062, Jackson ImmunoResearch Laboratories). Eps8, epidermal growth factor receptor pathway substrate 8; GAPDH, glyceraldehyde 3-phosphate dehydrogenase.

assessed using an Agilent 2100 Bioanalyzer and an RNA 6000 Nano Total RNA kit (both from Agilent Technologies, Inc.). Quantitative mRNA levels were determined using real-time RT-PCR using the Applied Biosystems 7900 HT Sequence Detection System, a TaqMan Gene Expression Assay for human EPS8 (assay ID Hs00610286_m1), and a Eukaryotic 18S rRNA Endogenous Control (Applied Biosystems; Thermo Fisher Scientific, Inc.). Only the probe sequence for EPS8 (TTGGATGAAAGCCAGAGCAGAGTGG) was provided by the manufacturer. The probes of EPS8 and 18S rRNA were labelled with FAM and VIC dyes, respectively. cDNA was generated using 100 ng of total RNA, and a High Capacity cDNA Reverse Transcription kit (Applied Biosystems; Thermo Fisher Scientific, Inc.). RT-PCR was carried out in a total volume of 20 μl containing 100 ng of cDNA, TaqMan Fast Advanced Master Mix (Applied Biosystems), and the respective TaqMan target gene reagents. The amplification conditions were 95˚C for 20 sec followed by 40 cycles of 95˚C for 1 sec and 60˚C for 20 sec. Samples were analyzed in triplicate as technical replicates. The EPS8 mRNA levels were defined from the cycle threshold (Ct), using the comparative Ct method (18), and each sample was normalized by comparison to 18S rRNA levels. The fold change of EPS8 mRNA levels in each cell line was determined using SU.86.86 cell EPS8 mRNA levels as a reference.

Statistical analysis. Student's t-test for comparison of cell motility between SU.86.86 and MIA PaCa-2 cell lines, the Pearson correlation coefficient to compare two variables in five analyses (exosomal Eps8 protein, intracellular Eps8 protein, intracellular Eps8 mRNA, migration, and invasion), and Multiple t-tests with Bonferroni-correction for comparison of three different cell origins of metastasis, ascites and primary tumors were used. P-values <0.05 were considered to indicate a statistically significant difference.

Results

In vitro migratory and invasive activities of SU.86.86 and MIA PaCa-2 cells. SU.86.86 cells were derived from a liver metastasis of a pancreatic ductal carcinoma (19). MIA PaCa-2 cells were derived from a primary pancreatic adenocarcinoma (20). Before proteome analysis, we first performed *in vitro* cell migration and invasion assays to evaluate if the two cell lines exhibited differences in metastatic-potential. The impedance-based RTCA has shown a strong correlation

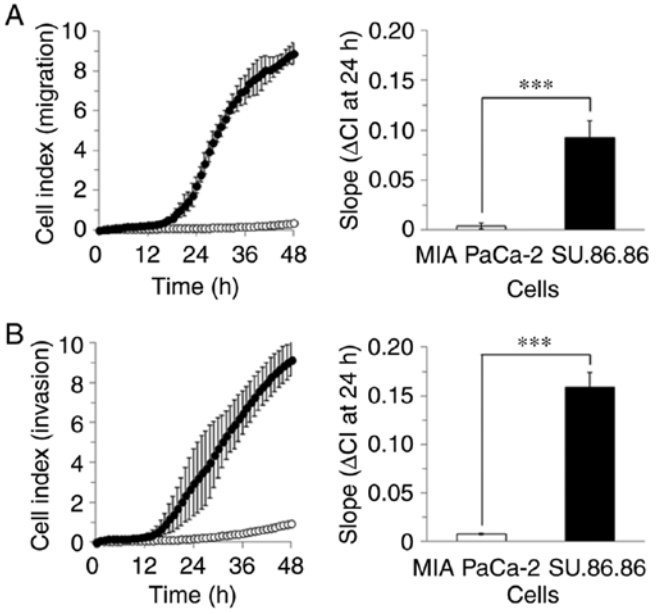

Figure 1. Real-time assessment of cell migration and invasion in human pancreatic cancer cell lines. Measurements were obtained for the metastasis-derived SU.86.86 and primary tumor-derived MIA PaCa-2 cell lines, using the xCELLigence RTCA DP instrument. Patterns of (A) cell migration and (B) invasion for SU.86.86 (closed circles) and MIA PaCa-2 (open circles) were reconstructed from the original data points by plotting data every hour. All data points are presented as the mean ± SD from independent quadruplicate (n=4) experiments. The kinetics for cell migration and invasion is presented as a linear slope of the cell index after 24 h. Statistical significance (***P<0.001) was evaluated using the Student's t-test.

with the conventional Boyden chamber Transwell endpoint assay (15,21). Using the RTCA assay system, SU.86.86 cells had 23-fold greater cell migratory activity than did MIA PaCa-2 cells (Fig. 1A). Additionally, using a Matrigel barrier, SU.86.86 cells were found to be 20-times more invasive than MIA PaCa-2 cells (Fig. 1B). Collectively, these results indicated that the *in vitro* cell migratory and invasive behaviors of SU.86.86 and MIA PaCa-2 cells were correlated with their metastatic and primary tumor cell origins, respectively.

Exosomal proteome profiles of SU.86.86 and MIA PaCa-2 cells. The proteome profiles of SU.86.86 and MIA PaCa-2 cell-derived exosomes were analyzed using LC-MS/MS. After 48 h of cell growth, exosomes were isolated from culture media by a series of filtration and ultracentrifugation steps as previ-

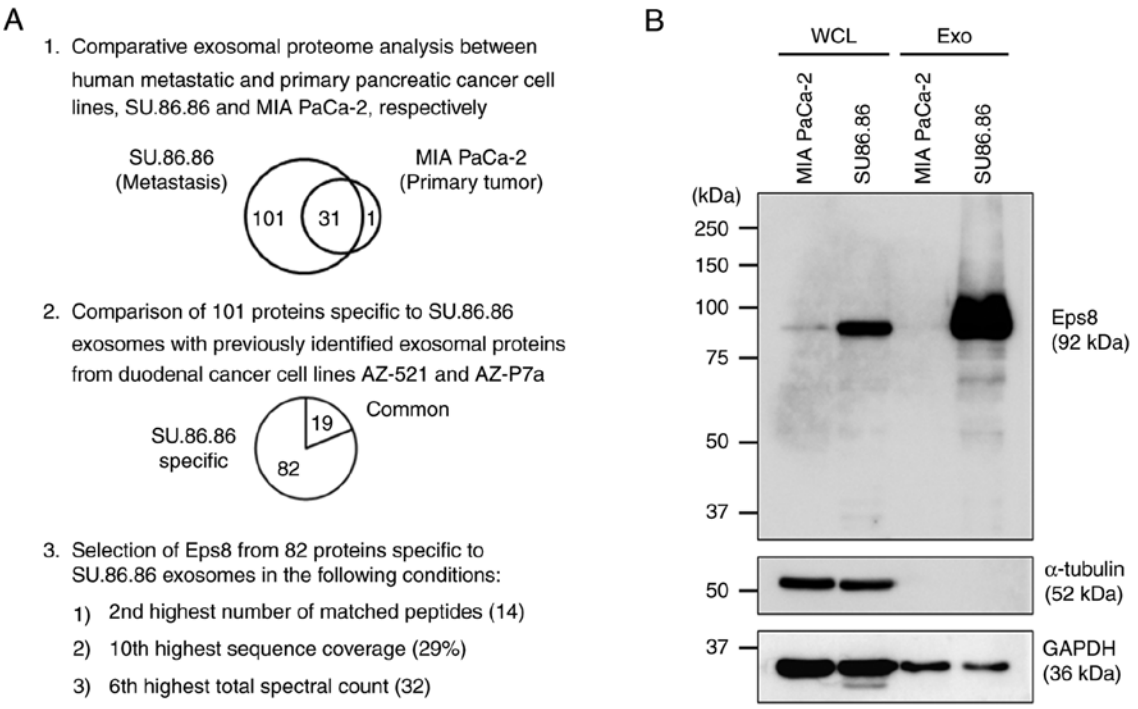

Figure 2. Identification of Eps8 in exosomes from SU.86.86 human metastatic pancreatic cancer cells by comparative proteomics. (A) The procedure was used to identify exosomal proteins specific to SU.86.86 cells. Comparison of proteins identified in SU.86.86-derived and MIA PaCa-2-derived exosomes revealed that 101 proteins were specifically observed in SU.86.86-derived exosomes (Venn diagram, step 1). All exosomal proteins derived from these two cell lines are listed in Table III. Comparison with proteins that had been previously identified in exosomes derived from duodenal cancer cell lines, AZ-521 and AZ-P7a (15) revealed that 82 from the 101 proteins aforementioned were specific to SU.86.86-derived exosomes (Pie chart, step 2). Comparative exosomal proteome data from the four cell lines are listed in Table IV. The Eps8 protein was selected as a specific exosomal protein derived from SU.86.86 in the indicated conditions (step 3). (B) Intracellular and exosomal Eps8 levels of SU.86.86 and MIA PaCa-2 cells. Proteins (10 mg) from WCL and Exo were separated by 8% SDS-PAGE and subjected to immunoblotting using antibodies against Eps8, α-tubulin, and GAPDH, the latter two of which were used as internal standards for WCL. For Exo, these two housekeeping proteins, α-tubulin and GAPDH, were not suitable for normalization (15), and no internal standard proteins were available. ESP8, epidermal growth factor receptor pathway substrate 8; WLC, whole cell lysates; Exo, exosomes.

ously described (15,16). Proteome data processing identified a total of 133 proteins from exosomes derived from both cell lines (Fig. 2A, Table III). Among them, 31 proteins were identified in the exosomes of both cell types. A total of 101 proteins were uniquely identified in SU.86.86 cell-derived exosomes, and a single unique protein, histone H2A type 2-B (H2A2B), was identified in MIA PaCa-2 cell-derived exosomes.

Identification of Eps8 in SU.86.86 cell-derived exosomes. To identify the SU.86.86 cell-specific exosomal proteins, we compared the 101 SU.86.86 cell-specific proteins with those that had been previously identified in exosomes derived from human duodenal cancer cell lines AZ-521 and AZ-P7a (Fig. 2A) (15). This comparison identified 82 proteins that were unique to SU.86.86 cell-derived exosomes (Table IV). Of the 82 proteins unique to SU.86.86, Eps8 revealed relatively high MS/MS values, including the number of matched peptides, the rate of sequence coverage, and the total spectral count. Furthermore, the Eps8 expression was elevated in pancreatic cancer cells derived from ascites and metastasis (22). Therefore, we chose to validate the presence of Eps8 in exosomes by western blot analysis.

Western blot analyses revealed that the Eps8 protein was abundant in SU.86.86 cell-derived exosomes, while no immunoreactive Eps8 signals were detected in MIA PaCa-2 cell-derived exosomes (Fig. 2B). Furthermore, intracellular Eps8 expression levels were much higher in SU.86.86 cells than in MIA PaCa-2 cells, indicating a positive correlation with tumor malignancy, as previously reported (22). Comparison of the house-keeping proteins in the exosomes of both cell types revealed variation in *glyceraldehyde* 3-phosphate dehydrogenase (GAPDH) levels and *no immunoreactive signals for* α-tubulin, making them unsuitable for normalizing exosomal protein levels previously described (15).

Exosomal Eps8 is abundant in metastasis- and ascites-derived pancreatic cancer cells. Eps8 was specifically detected in exosomes from metastatic-derived SU.86.86 cells. Therefore, we assessed exosomal Eps8 protein levels in other pancreatic cancer cell lines. Western blot analysis revealed positive immunoreactive Eps8 signals in exosomes from metastasis-derived pancreatic cancer cell lines, including CFPAC-1, KP-3, PK-45H, PK-8 and Capan-1 (Fig. 3A). Additionally, positive immunoreactive Eps8 signals were observed in exosomes from ascites-derived pancreatic cancer cell lines, including HuP-T3, HuP-T4 and AsPC-1. In contrast, Capan-2 was the only primary tumor cell line that exhibited Eps8 immunoreactivity. Densitometric analysis, using relative amounts of exosomal Eps8 protein, was used to quantify the Eps8 immunoreactivities observed (Fig. 4). The level of Eps8 immunoreactivity in the exosomes of different cell lines was assessed relative to that observed in SU.86.86 cell-derived exosomes, which was given a value of 1.0. The relative Eps8 immunoreactivity was 0.76, 0.15 and 0.17 in metastatic cell lines PK-45H, CFPAC-1

Table III. List of proteins identified in exosomes derived from SU.86.86 and MIA PaCa-2 cells.

Accession no.	UniProtKB/Swiss-Prot entry name	Protein name	M.W. (kDa)	Number of matched peptides	
				SU.86.86	MIA PaCa-2
Q7Z406	MYH14_HUMAN	Myosin-14	228	29	0
Q12929	EPS8_HUMAN	Epidermal growth factor receptor pathway substrate 8	92	14	0
Q14764	MVP_HUMAN	Major vault protein	99	14	0
P05121	PAI1_HUMAN	Plasminogen activator inhibitor 1	45	10	0
P16104	H2AX_HUMAN	Histone H2AX	15	8	0
P21589	5NTD_HUMAN	5'-nucleotidase	63	7	0
P84243	H33_HUMAN	Histone H3.3	15	7	0
Q9GZM7	TINAL_HUMAN	Tubulointerstitial nephritis antigen-like	52	7	0
P01023	A2MG_HUMAN	Alpha-2-macroglobulin	163	6	0
P80188	NGAL_HUMAN	Neutrophil gelatinase-associated lipocalin	23	6	0
P23396	RS3_HUMAN	40S ribosomal protein S3	27	5	0
Q9UQB8	BAIP2_HUMAN	Brain-specific angiogenesis inhibitor 1-associated protein 2	61	5	0
Q9UHR4	BI2L1_HUMAN	Brain-specific angiogenesis inhibitor 1-associated protein 2-like protein 1	57	5	0
P02458	CO2A1_HUMAN	Collagen alpha-1 (II) chain	142	5	0
P23142	FBLN1_HUMAN	Fibulin-1	77	5	0
P13647	K2C5_HUMAN	Keratin, type II cytoskeletal 5	62	5	0
P05787	K2C8_HUMAN	Keratin, type II cytoskeletal 8	54	5	0
P15880	RS2_HUMAN	40S ribosomal protein S2	31	4	0
P08865	RSSA_HUMAN	40S ribosomal protein SA	33	4	0
P09525	ANXA4_HUMAN	Annexin A4	36	4	0
P08133	ANXA6_HUMAN	Annexin A6	76	4	0
O95994	AGR2_HUMAN	Anterior gradient protein 2 homolog	20	4	0
O15335	CHAD_HUMAN	Chondroadherin	40	4	0
P12109	CO6A1_HUMAN	Collagen alpha-1 (VI) chain	109	4	0
P39060	COIA1_HUMAN	Collagen alpha-1 (XVIII) chain	178	4	0
P08238	HS90B_HUMAN	Heat shock protein HSP 90-beta	83	4	0
Q16270	IBP7_HUMAN	Insulin-like growth factor-binding protein 7	29	4	0
Q08431	MFGM_HUMAN	Lactadherin	43	4	0
Q13753	LAMC2_HUMAN	Laminin subunit gamma-2	131	4	0
Q9NRN5	OLFL3_HUMAN	Olfactomedin-like protein 3	46	4	0
O00391	QSOX1_HUMAN	Sulfhydryl oxidase 1	83	4	0
P00750	TPA_HUMAN	Tissue-type plasminogen activator	63	4	0
P29144	TPP2_HUMAN	Tripeptidyl-peptidase 2	138	4	0
Q9H9H4	VP37B_HUMAN	Vacuolar protein sorting-associated protein 37B	31	4	0
P62241	RS8_HUMAN	40S ribosomal protein S8	24	3	0
P46781	RS9_HUMAN	40S ribosomal protein S9	23	3	0
Q07020	RL18_HUMAN	60S ribosomal protein L18	22	3	0
P12429	ANXA3_HUMAN	Annexin A3	36	3	0
O75531	BAF_HUMAN	Barrier-to-autointegration factor	10	3	0
P02462	CO4A1_HUMAN	Collagen alpha-1(IV) chain	161	3	0
Q86YQ8	CPNE8_HUMAN	Copine-8	63	3	0

Table III. Continued.

Accession no.	UniProtKB/Swiss-Prot entry name	Protein name	M.W. (kDa)	Number of matched peptides	
				SU.86.86	MIA PaCa-2
P68871	HBB_HUMAN	Hemoglobin subunit beta	16	3	0
P16403	H12_HUMAN	Histone H1.2	21	3	0
Q71UI9	H2AV_HUMAN	Histone H2A.V	14	3	0
Q6ZNF0	ACP7_HUMAN	Acid phosphatase type 7	50	3	0
P02533	K1C14_HUMAN	Keratin, type I cytoskeletal 14	52	3	0
P05783	K1C18_HUMAN	Keratin, type I cytoskeletal 18	48	3	0
P04259	K2C6B_HUMAN	Keratin, type II cytoskeletal 6B	60	3	0
Q16787	LAMA3_HUMAN	Laminin subunit alpha-3	367	3	0
P60660	MYL6_HUMAN	Myosin light polypeptide 6	17	3	0
P19105	ML12A_HUMAN	Myosin regulatory light chain 12A	20	3	0
P19338	NUCL_HUMAN	Nucleolin	77	3	0
Q8WUM4	PDC6I_HUMAN	Programmed cell death 6-interacting protein	96	3	0
P00734	THRB_HUMAN	Prothrombin	70	3	0
P78371	TCPB_HUMAN	T-complex protein 1 subunit beta	57	3	0
P68371	TBB4B_HUMAN	Tubulin beta-4B chain	50	3	0
P62195	PRS8_HUMAN	26S protease regulatory subunit 8	46	2	0
P62847	RS24_HUMAN	40S ribosomal protein S24	15	2	0
P50914	RL14_HUMAN	60S ribosomal protein L14	23	2	0
P61313	RL15_HUMAN	60S ribosomal protein L15	24	2	0
P18124	RL7_HUMAN	60S ribosomal protein L7	29	2	0
P62424	RL7A_HUMAN	60S ribosomal protein L7a	30	2	0
P53999	TCP4_HUMAN	Activated RNA polymerase II transcriptional coactivator p15	14	2	0
P08758	ANXA5_HUMAN	Annexin A5	36	2	0
P98160	PGBM_HUMAN	Basement membrane-specific heparan sulfate proteoglycan core protein	469	2	0
P02749	APOH_HUMAN	Beta-2-glycoprotein 1	38	2	0
P62158	CALM_HUMAN	Calmodulin	17	2	0
P15169	CBPN_HUMAN	Carboxypeptidase N catalytic chain	52	2	0
P49747	COMP_HUMAN	Cartilage oligomeric matrix protein	83	2	0
Q9NZZ3	CHMP5_HUMAN	Charged multivesicular body protein 5	25	2	0
P08123	CO1A2_HUMAN	Collagen alpha-2(I) chain	129	2	0
P01031	CO5_HUMAN	Complement C5	188	2	0
O75367	H2AY_HUMAN	Core histone macro-H2A.1	40	2	0
P26641	EF1G_HUMAN	Elongation factor 1-gamma	50	2	0
Q9H6S3	ES8L2_HUMAN	Epidermal growth factor receptor kinase substrate 8-like protein 2	81	2	0
P09972	ALDOC_HUMAN	Fructose-bisphosphate aldolase C	39	2	0
P23229	ITA6_HUMAN	Integrin alpha-6	127	2	0
Q7Z794	K2C1B_HUMAN	Keratin, type II cytoskeletal 1b	62	2	0
P19013	K2C4_HUMAN	Keratin, type II cytoskeletal 4	57	2	0
P02538	K2C6A_HUMAN	Keratin, type II cytoskeletal 6A	60	2	0
P08729	K2C7_HUMAN	Keratin, type II cytoskeletal 7	51	2	0
P51884	LUM_HUMAN	Lumican	38	2	0
Q14112	NID2_HUMAN	Nidogen-2	151	2	0
P30101	PDIA3_HUMAN	Protein disulfide-isomerase A3	57	2	0
P60903	S10AA_HUMAN	Protein S100-A10	11	2	0
P31949	S10AB_HUMAN	Protein S100-A11	12	2	0

Table III. Continued.

Accession no.	UniProtKB/Swiss-Prot entry name	Protein name	M.W. (kDa)	Number of matched peptides	
				SU.86.86	MIA PaCa-2
P21980	TGM2_HUMAN	Protein-glutamine gamma-glutamyltransferase 2	77	2	0
Q92954	PRG4_HUMAN	Proteoglycan 4	151	2	0
P50454	SERPH_HUMAN	Serpin H1	46	2	0
P24821	TENA_HUMAN	Tenascin	241	2	0
P35908	K22E_HUMAN	Keratin, type II cytoskeletal 2 epidermal	65	16	1
P07437	TBB5_HUMAN	Tubulin beta chain	50	15	1
P0C0L4	CO4A_HUMAN	Complement C4-A	193	9	1
P35580	MYH10_HUMAN	Myosin-10	229	9	1
P68363	TBA1B_HUMAN	Tubulin alpha-1B chain	50	7	1
P36955	PEDF_HUMAN	Pigment epithelium-derived factor	46	6	1
P16401	H15_HUMAN	Histone H1.5	23	5	1
P23284	PPIB_HUMAN	Peptidyl-prolyl cis-trans isomerase B	24	5	1
Q9H444	CHM4B_HUMAN	Charged multivesicular body protein 4b	25	4	1
P05452	TETN_HUMAN	Tetranectin	23	4	1
P62854	RS26_HUMAN	40S ribosomal protein S26	13	2	1
P35579	MYH9_HUMAN	Myosin-9	227	78	11
P02751	FINC_HUMAN	Fibronectin	263	42	5
P04264	K2C1_HUMAN	Keratin, type II cytoskeletal 1	66	29	9
P07996	TSP1_HUMAN	Thrombospondin-1	129	27	2
P13645	K1C10_HUMAN	Keratin, type I cytoskeletal 10	59	26	4
P35527	K1C9_HUMAN	Keratin, type I cytoskeletal 9	62	19	2
P01024	CO3_HUMAN	Complement C3	187	17	2
P60709	ACTB_HUMAN	Actin, cytoplasmic 1	42	15	4
P07355	ANXA2_HUMAN	Annexin A2	39	14	2
P11142	HSP7C_HUMAN	Heat shock cognate 71 kDa protein	71	13	13
P15311	EZRI_HUMAN	Ezrin	69	13	6
P62805	H4_HUMAN	Histone H4	11	10	6
P04406	G3P_HUMAN	Glyceraldehyde-3-phosphate dehydrogenase	36	10	3
P06396	GELS_HUMAN	Gelsolin	86	10	2
P12259	FA5_HUMAN	Coagulation factor V	252	9	4
P14618	KPYM_HUMAN	Pyruvate kinase PKM	58	9	3
O00560	SDCB1_HUMAN	Syntenin-1	32	9	2
P33778	H2B1B_HUMAN	Histone H2B type 1-B	14	8	3
P04083	ANXA1_HUMAN	Annexin A1	39	8	2
P69905	HBA_HUMAN	Hemoglobin subunit alpha	15	6	3
P02768	ALBU_HUMAN	Serum albumin	69	5	4
P68104	EF1A1_HUMAN	Elongation factor 1-alpha 1	50	5	3
P04075	ALDOA_HUMAN	Fructose-bisphosphate aldolase A	39	5	3
P06733	ENOA_HUMAN	Alpha-enolase	47	4	2
P03956	MMP1_HUMAN	Interstitial collagenase	54	4	2
P02788	TRFL_HUMAN	Lactotransferrin	78	2	5
P62249	RS16_HUMAN	40S ribosomal protein S16	16	2	4
P10643	CO7_HUMAN	Complement component C7	94	2	3
P02748	CO9_HUMAN	Complement component C9	63	2	3
Q71DI3	H32_HUMAN	Histone H3.2	15	2	2
Q06830	PRDX1_HUMAN	Peroxiredoxin-1	22	2	2
Q8IUE6	H2A2B_HUMAN	Histone H2A type 2-B	14	0	3

Table IV. List of proteins specifically identified in exosomes derived from SU.86.86 compared to other cancer cell lines.

Accession no.	UniProtKB/Swiss-Prot entry name	Protein name	M.W. (kDa)	Number of matched peptides	Sequence coverage (%)	Total spectral count
Q7Z406	MYH14_HUMAN	Myosin-14	228	29	19	71
Q12929	EPS8_HUMAN	Epidermal growth factor receptor pathway substrate 8	92	14	29	32
Q14764	MVP_HUMAN	Major vault protein	99	14	25	27
P05121	PAI1_HUMAN	Plasminogen activator inhibitor 1	45	10	31	28
P16104	H2AX_HUMAN	Histone H2AX	15	8	52	46
P84243	H33_HUMAN	Histone H3.3	15	7	52	28
Q9GZM7	TINAL_HUMAN	Tubulointerstitial nephritis antigen-like	52	7	21	18
P21589	5NTD_HUMAN	5'-nucleotidase	63	7	17	15
P80188	NGAL_HUMAN	Neutrophil gelatinase-associated lipocalin	23	6	44	24
P36955	PEDF_HUMAN	Pigment epithelium-derived factor	46	6	17	13
P23284	PPIB_HUMAN	Peptidyl-prolyl cis-trans isomerase B	24	5	29	14
P13647	K2C5_HUMAN	Keratin, type II cytoskeletal 5	62	5	17	22
P05787	K2C8_HUMAN	Keratin, type II cytoskeletal 8	54	5	16	15
P16401	H15_HUMAN	Histone H1.5	23	5	16	13
Q9UQB8	BAIP2_HUMAN	Brain-specific angiogenesis inhibitor 1-associated protein 2	61	5	15	6
Q9UHR4	BI2L1_HUMAN	Brain-specific angiogenesis inhibitor 1-associated protein 2-like protein 1	57	5	14	16
P23142	FBLN1_HUMAN	Fibulin-1	77	5	6	13
P02458	CO2A1_HUMAN	Collagen alpha-1 (II) chain	142	5	4	13
O95994	AGR2_HUMAN	Anterior gradient protein 2 homolog	20	4	30	5
Q9H444	CHM4B_HUMAN	Charged multivesicular body protein 4b	25	4	22	7
Q9H9H4	VP37B_HUMAN	Vacuolar protein sorting-associated protein 37B	31	4	22	4
P08865	RSSA_HUMAN	40S ribosomal protein SA	33	4	21	6
O15335	CHAD_HUMAN	Chondroadherin	40	4	16	8
P09525	ANXA4_HUMAN	Annexin A4	36	4	16	5
Q16270	IBP7_HUMAN	Insulin-like growth factor-binding protein 7	29	4	15	11
Q08431	MFGM_HUMAN	Lactadherin	43	4	13	4
P00750	TPA_HUMAN	Tissue-type plasminogen activator	63	4	11	8
P08133	ANXA6_HUMAN	Annexin A6	76	4	9	4
O00391	QSOX1_HUMAN	Sulfhydryl oxidase 1	83	4	6	7
P12109	CO6A1_HUMAN	Collagen alpha-1 (VI) chain	109	4	5	7
Q13753	LAMC2_HUMAN	Laminin subunit gamma-2	131	4	5	8
P29144	TPP2_HUMAN	Tripeptidyl-peptidase 2	138	4	5	4
P39060	COIA1_HUMAN	Collagen alpha-1 (XVIII) chain	178	4	4	6
O75531	BAF_HUMAN	Barrier-to-autointegration factor	10	3	43	5
P68371	TBB4B_HUMAN	Tubulin beta-4B chain	50	3	41	45
Q71UI9	H2AV_HUMAN	Histone H2A.V	14	3	31	25
P19105	ML12A_HUMAN	Myosin regulatory light chain 12A	20	3	27	3
P60660	MYL6_HUMAN	Myosin light polypeptide 6	17	3	24	7

Table IV. Continued.

Accession no.	UniProtKB/Swiss-Prot entry name	Protein name	M.W. (kDa)	Number of matched peptides	Sequence coverage (%)	Total spectral count
P02533	K1C14_HUMAN	Keratin, type I cytoskeletal 14	52	3	18	40
P12429	ANXA3_HUMAN	Annexin A3	36	3	14	3
P05783	K1C18_HUMAN	Keratin, type I cytoskeletal 18	48	3	13	7
P04259	K2C6B_HUMAN	Keratin, type II cytoskeletal 6B	60	3	12	38
P46781	RS9_HUMAN	40S ribosomal protein S9	23	3	12	6
Q6ZNF0	ACP7_HUMAN	Acid phosphatase type 7	50	3	12	5
P78371	TCPB_HUMAN	T-complex protein 1 subunit beta	57	3	11	3
Q86YQ8	CPNE8_HUMAN	Copine-8	63	3	8	3
P19338	NUCL_HUMAN	Nucleolin	77	3	6	9
Q16787	LAMA3_HUMAN	Laminin subunit alpha-3	367	3	3	3
P02462	CO4A1_HUMAN	Collagen alpha-1(IV) chain	161	3	2	5
P60903	S10AA_HUMAN	Protein S100-A10	11	2	35	4
P62158	CALM_HUMAN	Calmodulin	17	2	26	5
P31949	S10AB_HUMAN	Protein S100-A11	12	2	24	4
P62854	RS26_HUMAN	40S ribosomal protein S26	13	2	21	12
P62847	RS24_HUMAN	40S ribosomal protein S24	15	2	20	7
Q9NZZ3	CHMP5_HUMAN	Charged multivesicular body protein 5	25	2	18	2
P02538	K2C6A_HUMAN	Keratin, type II cytoskeletal 6A	60	2	13	25
P09972	ALDOC_HUMAN	Fructose-bisphosphate aldolase C	39	2	13	4
O75367	H2AY_HUMAN	Core histone macro-H2A.1	40	2	12	6
P53999	TCP4_HUMAN	Activated RNA polymerase II transcriptional coactivator p15	14	2	12	4
P18124	RL7_HUMAN	60S ribosomal protein L7	29	2	10	3
P08758	ANXA5_HUMAN	Annexin A5	36	2	10	3
P19013	K2C4_HUMAN	Keratin, type II cytoskeletal 4	57	2	8	13
P62424	RL7A_HUMAN	60S ribosomal protein L7a	30	2	7	6
P08729	K2C7_HUMAN	Keratin, type II cytoskeletal 7	51	2	7	11
P62195	PRS8_HUMAN	26S protease regulatory subunit 8	46	2	7	2
P50454	SERPH_HUMAN	Serpin H1	46	2	7	2
P51884	LUM_HUMAN	Lumican	38	2	7	4
Q7Z794	K2C1B_HUMAN	Keratin, type II cytoskeletal 1b	62	2	7	21
P15169	CBPN_HUMAN	Carboxypeptidase N catalytic chain	52	2	6	2
P26641	EF1G_HUMAN	Elongation factor 1-gamma	50	2	6	4
P02749	APOH_HUMAN	Beta-2-glycoprotein 1	38	2	5	4
P30101	PDIA3_HUMAN	Protein disulfide-isomerase A3	57	2	5	3
P21980	TGM2_HUMAN	Protein-glutamine gamma-glutamyltransferase 2	77	2	4	5
P49747	COMP_HUMAN	Cartilage oligomeric matrix protein	83	2	4	4
Q9H6S3	ES8L2_HUMAN	Epidermal growth factor receptor kinase substrate 8-like protein 2	81	2	4	3
P23229	ITA6_HUMAN	Integrin alpha-6	127	2	3	2
Q14112	NID2_HUMAN	Nidogen-2	151	2	2	3
Q92954	PRG4_HUMAN	Proteoglycan 4	151	2	2	10
P08123	CO1A2_HUMAN	Collagen alpha-2(I) chain	129	2	2	3
P01031	CO5_HUMAN	Complement C5	188	2	1	3
P24821	TENA_HUMAN	Tenascin	241	2	1	2
P98160	PGBM_HUMAN	Basement membrane-specific heparan sulfate proteoglycan core protein	469	2	0	3

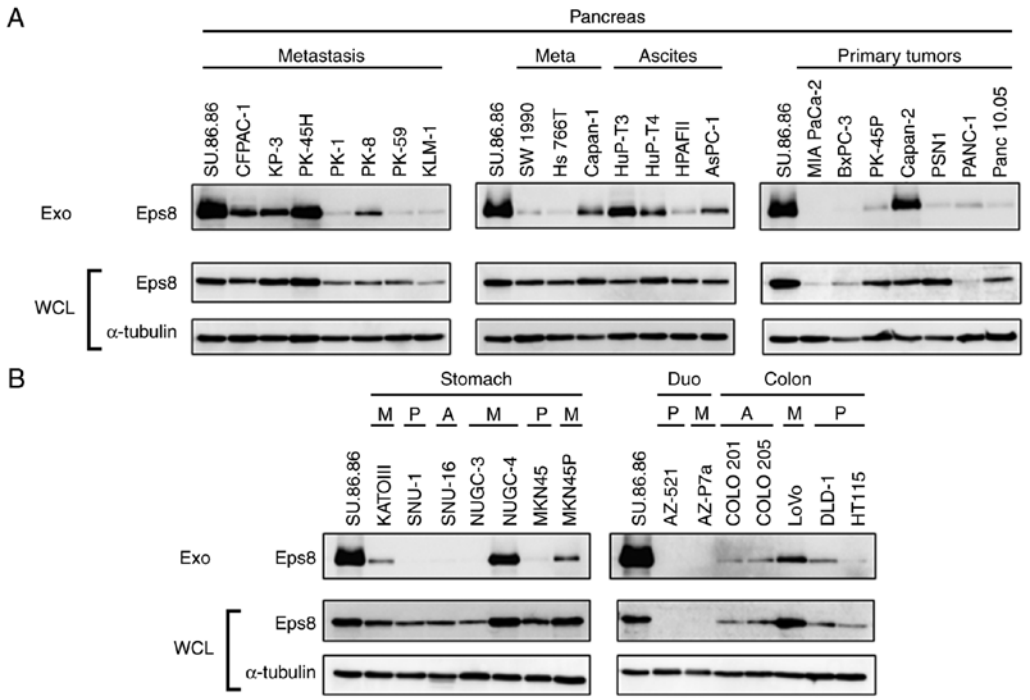

Figure 3. Exosomal and intracellular Eps8 protein levels in cancer cell lines. (A) Exosomal and intracellular Eps8 levels in pancreatic cancer cell lines derived from metastasis (Meta, M), ascites (A) and primary tumors (P). (B) Exosomal and intracellular Eps8 levels in cancer cell lines derived from stomach, duodenum and colon. Proteins (5 mg) from WCL and exosomes Exo were separated by 8% SDS-PAGE followed by immunoblotting using a mouse monoclonal Eps8 antibody. α-tubulin protein levels were measured as internal standards. ESP8, epidermal growth factor receptor pathway substrate 8; WLC, whole cell lysates; Exo, exosomes.

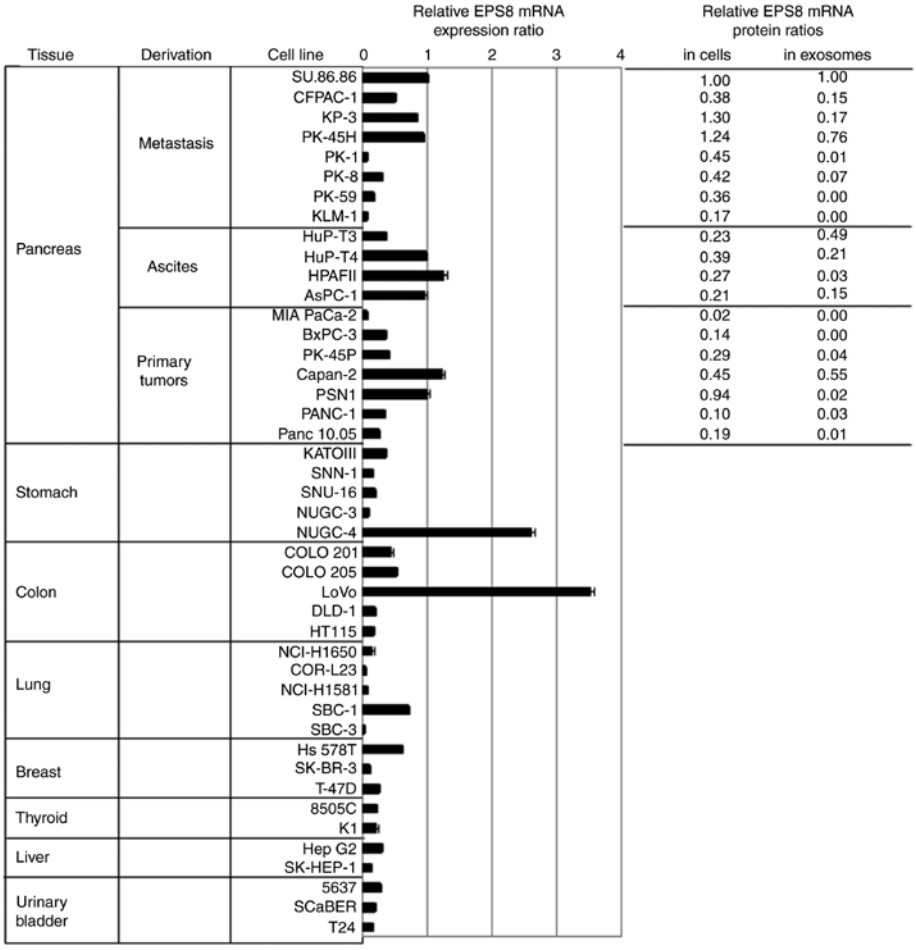

Figure 4. Intracellular EPS8 mRNA levels in cancer cell lines. EPS8 mRNA levels in cancer cell lines relative to the levels assessed in SU.86.86 cells are presented. Relative intracellular and exosomal Eps8 protein levels are presented on the right side. ESP8, epidermal growth factor receptor pathway substrate 8.

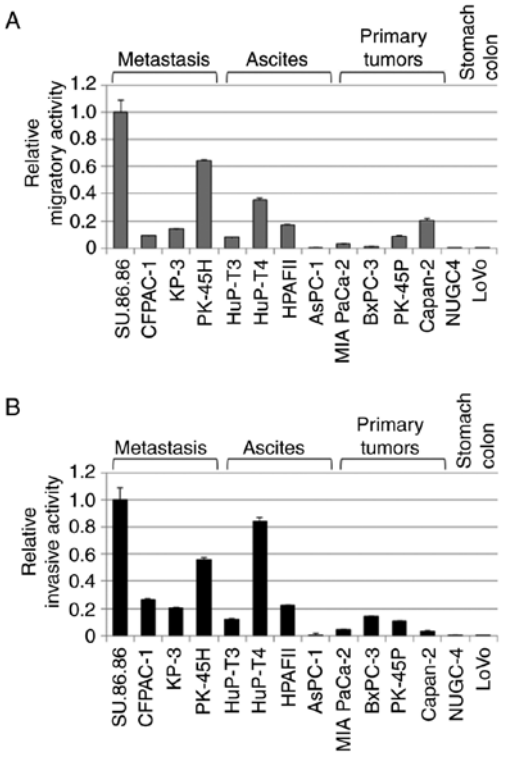

Figure 5. Cell migratory and invasive activities in pancreatic cancer cell lines. Relative activities of (A) cell migration and (B) invasion among cancer cell lines are presented relative to the activities observed in SU.86.86 cells. NUGC-4 cells derived from stomach cancer and LoVo cells from colon cancer were examined as these cells exhibited moderate levels of exosomal Eps8 immunoreactivity. ESP8, epidermal growth factor receptor pathway substrate 8.

and KP-3, respectively. In ascites-derived cell lines HuP-T3, HuP-T4, and AsPC-1, and the Capan-2 primary tumor cell line, the relative Eps8 immunoreactivity was 0.49, 0.21, 0.15 and 0.55, respectively. Intracellular Eps8 levels varied among the cell lines, particularly those derived from metastasis (PK-1, PK-8, PK-59 and KLM-1) and primary tumors (MIA PaCa-2, BxPC-3, PANC-1 and Panc 10.05). Except for PK-8, there was either no Eps8 immunoreactivity, or less Eps8 immunoreactivity, relative to that observed intracellularly, observed in the exosomes of these cells. Also, distinct Eps8 immunoreactivity was observed in NUGC-4 and MKN45P stomach cancer cell lines and the LoVo colon cancer cell line (Fig. 3B). Furthermore, cells with relatively high intracellular Eps8 protein levels expressed greater amounts of EPS8 mRNA (Fig. 4). However, Eps8 protein and mRNA expression levels did not correlate with the amount of Eps8 in exosomes. Collectively, these results revealed that, particularly in pancreatic cancer cells derived from metastasis and ascites, Eps8 was secreted into the extracellular environment via exosomes.

In vitro migratory and invasive activities of pancreatic cancer cell lines. It was revealed that Eps8 protein is present in the exosomes of several pancreatic cancer cell lines in addition to SU.86.86. Therefore, we evaluated the *in vitro* cell migratory and invasive activities in 12 pancreatic cancer cell lines. The highest levels of migratory and invasive activities were observed in SU.86.86 cells, and these were set at a value of 1 to allow for comparison (Fig. 5). The metastatic PK-45H cell line, with the relative exosomal Eps8 protein level of 0.76, revealed relatively high levels of cell migratory (0.64) and invasive activities (0.56). Additionally, in ascites-derived HuP-T4 cells, with the relative exosomal Eps8 protein level of 0.21, relatively high levels of cell migratory (0.36) and invasive activities (0.84) were observed. However, no cell motility was detected in stomach cancer-derived NUGC-4 cells and colon cancer-derived LoVo cells, which exhibited moderate levels of exosomal Eps8 immunoreactivities (Fig. 3).

Integrative comparison of the data revealed that similar to SU.86.86 cells, PK-45H cells consistently had the highest levels of *in vitro* cell migratory and invasive activities, exosomal and intracellular Eps8 protein, and EPS8 mRNA expression (Fig. 6A and B). Furthermore, using the Pearson correlation coefficient, we identified that exosomal Eps8 levels were significantly correlated with migratory cell levels ($r=0.85$, $P=4.2x10^{-4}$) (Fig. 6C). Therefore, we proposed that exosomal Eps8 protein level is indicative of metastatic potential in human pancreatic cancer cells.

Discussion

The present study revealed abundant levels of Eps8 protein in exosomes derived from pancreatic cancer cell lines. Furthermore, it was revealed that exosomal Eps8 levels were significantly correlated with migratory cell potential (Fig. 6C). Eps8 was initially identified as a substrate for the epidermal growth factor (EGF) receptor that enhances EGF-dependent mitogenic signals (23,24). Overexpression of Eps8 has been revealed to promote cellular proliferation and/or migration in various tumor types, including breast cancer (25), malignant glioma (26,27), pituitary tumors (28), oral squamous cell carcinoma (29), and cervical cancer (30). In Eps8-mediated tumorigenesis and proliferation, stimulated EGFR results in the activation of downstream pathways, including Eps8/Ras/MAPK, Eps8/Akt/FoxM1 and Eps8/mTOR/STAT3 were revealed (31).

Eps8 expression was enhanced in pancreatic cancer at both protein and mRNA levels (22), and Eps8 upregulation was immunohistochemically detected in 72% of paraffin-embedded clinical specimens (32). Welsch *et al* demonstrated that Eps8 expression levels were correlated with the degree of malignancy in pancreatic cancer cell lines (22). They found low levels of Eps8 expression in cell lines from primary pancreatic cancers (MIAPaCa-2, BxPC-3, and PANC-1), moderate Eps8 expression levels in cell lines from metastasis (SU.86.86 and Capan-1), and high Eps8 expression level in a cell line from malignant ascites (AsPC-1) (22). Additionally, their Eps8 expression levels were positively correlated with migratory potential (BxPC-3 < PANC-1<Capan-1<AsPC-1). In the present study, a moderate correlation between cell migratory capacity and intracellular Eps8 protein expression levels ($r=0.65$, $P=2.0x10^{-2}$) was revealed but not between cell migratory capacity and intracellular EPS8 mRNA expression levels ($r=0.44$, $P=1.5x10^{-1}$) (Fig. 6C). However, we identified a significant correlation between exosomal Eps8 protein levels and migratory cell capacity ($r=0.85$, $P=4.2x10^{-4}$). The pancreatic cancer cell lines that exhibited relatively high exosomal Eps8 protein levels were SU.86.86 and PK-45H from metastasis, HuP-T3 from ascites, and Capan-2 from

A

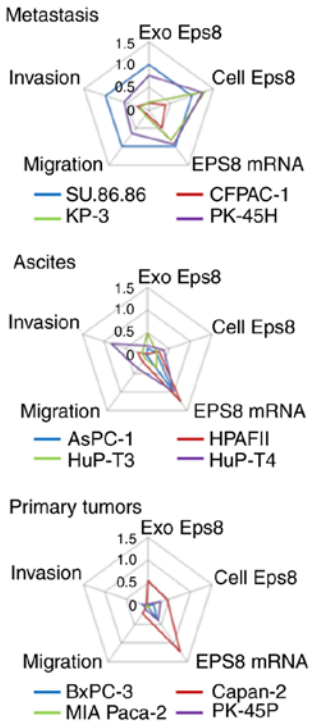

B

		Relative ratio of Eps8			Relative ratio	
		Protein in Exo	Protein in cells	mRNA in cells	Migration	Invasion
Metastasis	SU.86.86	1.00	1.00	1.00	1.00	1.00
	CFPAC-1	0.15	0.38	0.49	0.09	0.27
	KP-3	0.17	1.30	0.84	0.14	0.21
	PK-45H	0.76	1.24	0.94	0.64	0.56
Ascites	AsPC-1	0.15	0.21	0.96	0.01	0.01
	HPAFII	0.03	0.27	1.26	0.17	0.23
	HuP-T3	0.49	0.23	0.34	0.08	0.12
	HuP-T4	0.21	0.39	0.97	0.36	0.84
Primary tumors	BxPC-3	NA	0.14	0.35	0.01	0.14
	Capan-2	0.55	0.45	1.23	0.20	0.04
	MIA PaCa-2	NA	0.02	0.05	0.03	0.05
	PK-45P	0.04	0.29	0.40	0.09	0.11

C

	Exo Eps8	Cell Eps8	Eps8 mRNA	Migration	Invasion
Exo Eps8	1	0.61 3.6×10^{-2}	0.40 2.0×10^{-1}	0.85 4.2×10^{-4}	0.60 3.7×10^{-2}
Cell Eps8	0.61 3.6×10^{-2}	1	0.43 1.6×10^{-1}	0.65 2.0×10^{-2}	0.51 9.2×10^{-2}
Eps8 mRNA	0.40 2.0×10^{-1}	0.43 1.6×10^{-1}	1	0.44 1.5×10^{-1}	0.35 2.6×10^{-1}
Migration	0.85 4.2×10^{-4}	0.65 2.0×10^{-2}	0.44 1.5×10^{-1}	1	0.87 2.0×10^{-4}
Invasion	0.60 3.7×10^{-2}	0.51 9.2×10^{-2}	0.35 2.6×10^{-1}	0.87 2.0×10^{-4}	1

Figure 6. Comparison of Eps8 levels in the exosomes and cells of pancreatic cancer cell lines. The cell motile activities of cell lines derived from metastasis, ascites, and primary tumors were compared. (A) Radar charts revealing relative Eps8 protein in exosomes and cells, Eps8 mRNA expression level, and cell migratory and invasive activities. (B) Relative Eps8 protein and mRNA levels and cell motility in pancreatic cancer cells and their exosomes. (C) Correlations between exosomal Eps8 protein level, intracellular Eps8 protein and mRNA levels, and cell migratory and invasive activities. Correlation coefficient r and P-values are represented by the upper and lower numbers in each cell. ESP8, epidermal growth factor receptor pathway substrate 8.

primary tumor cells (Figs. 3A and 6B). Despite originating from primary tumor cells, Capan-2 exhibited moderate cell migratory activity (Figs. 5A and 6B). These results were consistent with those revealing that Capan-2 possessed metastatic potential to the liver after being inoculated into nude mice (33). AsPC-1 cells, derived from ascites, have been previously revealed to have intracellular Eps8 protein and mRNA expression levels and migratory cell potential greater than those of metastasis-derived SU.86.86 cells (22). In our study, AsPC-1 cells had lower levels of intracellular and exosomal Eps8 protein and migratory cell levels than did SU.86.86 cells (Figs. 3A, 5A and 6B). We assume that these different results for AsPC-1 cells are at least due to culture conditions for maintenance of the cell line and preparation of samples. Additionally, among three groups of pancreatic cancer cell lines with different degrees of malignancy, intracellular Eps8 expression levels were significantly higher in cells from metastasis than in those from ascites (P=0.01628, the Bonferroni-corrected threshold for multiple t-tests =0.01667, α=0.05). Eps8 expression in ascites-derived cell lines did not significantly differ from that of primary tumor-derived cell lines (P=0.634). Eps8 expression levels in metastasis-derived cell lines were significantly higher than in primary tumor-derived cell lines (P=0.01662). We compared the levels of exosomal Eps8 protein, intracellular Eps8 mRNA, migratory and invasive activities of metastasis-, ascites-, and primary tumor-derived cell line groups and found no significant differences. Therefore, the present study indicated that there is a strong relationship between exosomal Eps8 protein level and migratory cell potential.

Exosomes play an essential role in tumor metastasis (34). Eps8 is involved in metastasis, and inhibiting Eps8 expression results in decreased levels of cell motility (26,30,32). The Eps8 protein localizes to lysosomes via the late endosomes, which function as a pre-degenerative compartment (35). The late endosomes also function as a recycling compartment, leading to extracellular secretion via fusion with the plasma membrane (1,36,37). Collectively, with the present results, it may be inferred that Eps8 protein is recruited to late endosomes, leading to either inclusion in lysosomes or extracellular secretion. Our results revealed that in pancreatic cancer cell lines with high migratory potential, Eps8 protein abundance in exosomes occurs through extracellular secretion. These observations indicated that exosomal Eps8 has a potential to be a metastatic biomarker for pancreatic cancer. Further studies need to be performed using clinical samples to validate this hypothesis. For validation, it is conceivable to use an ELISA system, which can easily detect secreted proteins in serum or plasma blood samples. For proteins embedded in exosomes, such as Eps8, it is challenging to develop an ELISA system, since detergents that may affect the assay are used for exosome lysis during the sample preparation.

Acknowledgements

Not applicable.

Funding

The present study was supported by the JSPS KAKENHI grant nos. JP26430150 and JP16K10523 to K.O.

Availability of data and materials

The datasets used during the present study are available from the corresponding author upon reasonable request.

Authors' contributions

KO made substantial contributions to the design of the study, drafting of the manuscript, cell culture and the preparation of the exosomes. KH, KWN and NS were responsible for the proteome analysis using LC-MS/MS. KK and TI performed the western blotting experiments. KK, YW and SM were involved in RNA preparation and RT-PCR analysis. KY and TM supervised the study and analyzed the data. All authors read and approved the manuscript and agree to be accountable for all aspects of the research in ensuring that the accuracy or integrity of any part of the work are appropriately investigated and resolved.

Ethics approval and consent to participate

This article contains no studies with human participants performed by any of the authors.

Patient consent for publication

Not applicable.

Competing interests

The authors declare that they have no competing interests.

References

1. Colombo M, Raposo G and Théry C: Biogenesis, secretion, and intercellular interactions of exosomes and other extracellular vesicles. Annu Rev Cell Dev Biol 30: 255-289, 2014.
2. Greening DW, Xu R, Gopal SK, Rai A and Simpson RJ: Proteomic insights into extracellular vesicle biology-defining exosomes and shed microvesicles. Expert Rev Proteomics 14: 69-95, 2007.
3. Kalluri R: The biology and function of exosomes in cancer. J Clin Invest 126: 1208-1215, 2016.
4. Soung YH, Ford S, Zhang V and Chung J: Exosomes in cancer diagnostics. Cancers 9: 8, 2017.
5. Choi DS, Kim DK, Kim YK and Gho YS: Proteomics, transcriptomics and lipidomics of exosomes and ectosomes. Proteomics 13: 1554-1571, 2013.
6. EL Andaloussi S, Mäger I, Breakefield XO and Wood MJ: Extracellular vesicles: Biology and emerging therapeutic opportunities. Nat Rev Drug Discov 12: 347-357, 2013.
7. Siegel RL, Miller KD and Jemal A: Cancer statistics, 2017. CA Cancer J Clin 67: 7-30, 2017.
8. Ferlay J, Partensky C and Bray F: More deaths from pancreatic cancer than breast cancer in the EU by 2017. Acta Oncol 55: 1158-1160, 2016.
9. Hanada K, Okazaki A, Hirano N, Izumi Y, Teraoka Y, Ikemoto J, Kanemitsu K, Hino F, Fukuda T and Yonehara S: Diagnostic strategies for early pancreatic cancer. J Gastroenterol 50: 147-154, 2015.
10. Nuzhat Z, Kinhal V, Sharma S, Rice GE, Joshi V and Salomon C: Tumour-derived exosomes as a signature of pancreatic cancer-liquid biopsies as indicators of tumour progression. Oncotarget 8: 17279-17291, 2017.
11. Le Large TYS, Bijlsma MF, Kazemier G, van Laarhoven HWM, Giovannetti E and Jimenez CR: Key biological processes driving metastatic spread of pancreatic cancer as identified by multi-omics studies. Semin Cancer Biol 44: 153-169, 2017.
12. Sasaki K, Sato K, Akiyama Y, Yanagihara K, Oka M and Yamaguchi K: Peptidomics-based approach reveals the secretion of the 29-residue COOH-terminal fragment of the putative tumor suppressor protein DMBT1 from pancreatic adenocarcinoma cell lines. Cancer Res 62: 4894-4898, 2002.
13. Ogura S, Kaneko K, Miyajima S, Ohshima K, Yamaguchi K and Mochizuki T: Proneurotensin/neuromedin N secreted from small cell lung carcinoma cell lines as a potential tumor marker. Proteomics Clin Appl 2: 1620-1627, 2008.
14. Valadi H, Ekström K, Bossios A, Sjöstrand M, Lee JJ and Lötvall JO: Exosome-mediated transfer of mRNAs and microRNAs is a novel mechanism of genetic exchange between cells. Nat Cell Biol 9: 654-659, 2007.
15. Ohshima K, Kanto K, Hatakeyama K, Ide T, Wakabayashi-Nakao K, Watanabe Y, Sakura N, Terashima M, Yamaguchi K and Mochizuki T: Exosome-mediated extracellular release of polyadenylate-binding protein 1 in human metastatic duodenal cancer cells. Proteomics 14: 2297-2306, 2014.
16. Ohshima K, Inoue K, Fujiwara A, Hatakeyama K, Kanto K, Watanabe Y, Muramatsu K, Fukuda Y, Ogura S, Yamaguchi K and Mochizuki T: Let-7 microRNA family is selectively secreted into the extracellular environment via exosomes in a metastatic gastric cancer cell line. PLoS One 5: e13247, 2010.
17. Hatakeyama K, Ohshima K, Fukuda Y, Ogura S, Terashima M, Yamaguchi K and Mochizuki T: Identification of a novel protein isoform derived from cancer-related splicing variants using combined analysis of transcriptome and proteome. Proteomics 11: 2275-2282, 2011.
18. Livak KJ and Schmittgen TD: Analysis of relative gene expression data using real-time quantitative PCR and the $2^{-\Delta\Delta C_T}$ method. Methods 25: 402-408, 2001.
19. Drucker BJ, Marincola FM, Siao DY, Donlon TA, Bangs CD and Holder WD Jr: A new human pancreatic carcinoma cell line developed for adoptive immunotherapy studies with lymphokine-activated killer cells in nude mice. In Vitro Cell Dev Biol 24: 1179-1187, 1988.
20. Yunis AA, Arimura GK and Russin DJ: Human pancreatic carcinoma (MIA PaCa-2) in continuous culture: Sensitivity to asparaginase. Int J Cancer 19: 128-135, 1977.
21. Limame R, Wouters A, Pauwels B, Fransen E, Peeters M, Lardon F, De Wever O and Pauwels P: Comparative analysis of dynamic cell viability, migration and invasion assessments by novel real-time technology and classic endpoint assays. PLoS One 7: e46536, 2012.
22. Welsch T, Endlich K, Giese T, Büchler MW and Schmidt J: Eps8 is increased in pancreatic cancer and required for dynamic actin-based cell protrusions and intercellular cytoskeletal organization. Cancer Lett 255: 205-218, 2007.
23. Fazioli F, Minichiello L, Matoska V, Castagnino P, Miki T, Wong WT and Di Fiore PP: Eps8, a substrate for the epidermal growth factor receptor kinase, enhances EGF-dependent mitogenic signals. EMBO J 12: 3799-3808, 1993.
24. Castagnino P, Biesova Z, Wong WT, Fazioli F, Gill GN and Di Fiore PP: Direct binding of eps8 to the juxtamembrane domain of EGFR is phosphotyrosine- and SH2-independent. Oncogene 10: 723-729, 1995.
25. Chen C, Liang Z, Huang W, Li X, Zhou F, Hu X, Han M, Ding X and Xiang S: Eps8 regulates cellular proliferation and migration of breast cancer. Int J Oncol 46: 205-214, 2015.
26. Cattaneo MG, Cappellini E and Vicentini LM: Silencing of Eps8 blocks migration and invasion in human glioblastoma cell lines. Exp Cell Res 318: 1901-1912, 2012.
27. Ding X, Zhou F, Wang F, Yang Z, Zhou C, Zhou J, Zhang B, Yang J, Wang G, Wei Z, *et al*: Eps8 promotes cellular growth of human malignant gliomas. Oncol Rep 29: 697-703, 2013.
28. Xu M, Shorts-Cary L, Knox AJ, Kleinsmidt-DeMasters B, Lillehei K and Wierman ME: Epidermal growth factor receptor pathway substrate 8 is overexpressed in human pituitary tumors: Role in proliferation and survival. Endocrinology 150: 2064-2071, 2009.
29. Yap LF, Jenei V, Robinson CM, Moutasim K, Benn TM, Threadgold SP, Lopes V, Wei W, Thomas GJ and Paterson IC: Upregulation of Eps8 in oral squamous cell carcinoma promotes cell migration and invasion through integrin-dependent Rac1 activation. Oncogene 28: 2524-2534, 2009.

30. Li Q, Bao W, Fan Q, Shi WJ, Li ZN, Xu Y and Wu D: Epidermal growth factor receptor kinase substrate 8 promotes the metastasis of cervical cancer via the epithelial-mesenchymal transition. Mol Med Rep 14: 3220-3228, 2016.
31. Li YH, Xue TY, He YZ and Du JW: Novel oncoprotein EPS8: A new target for anticancer therapy. Future Oncol 9: 1587-1594, 2013.
32. Tod J, Hanley CJ, Morgan MR, Rucka M, Mellows T, Lopez MA, Kiely P, Moutasim KA, Frampton SJ, Sabnis D, *et al*: Pro-migratory and TGF-β-activating functions of αvβ6 integrin in pancreatic cancer are differentially regulated via an Eps8-dependent GTPase switch. J Pathol 243: 37-50, 2017.
33. Uchima Y, Sawada T, Nishihara T, Maeda K, Ohira M and Hirakawa K: Inhibition and mechanism of action of a protease inhibitor in human pancreatic cancer cells. Pancreas 29: 123-131, 2004.
34. Peinado H, Zhang H, Matei IR, Costa-Silva B, Hoshino A, Rodrigues G, Psaila B, Kaplan RN, Bromberg JF, Kang Y, *et al*: Pre-metastatic niches: Organ-specific homes for metastases. Nat Rev Cancer 17: 302-317, 2017.
35. Welsch T, Younsi A, Disanza A, Rodriguez JA, Cuervo AM, Scita G and Schmidt J: Eps8 is recruited to lysosomes and subjected to chaperone-mediated autophagy in cancer cells. Exp Cell Res 316: 1914-1924, 2010.
36. Théry C, Zitvogel L and Amigorena S: Exosomes: Composition, biogenesis and function. Nat Rev Immunol 2: 569-579, 2002.
37. Théry C, Ostrowski M and Segura E: Membrane vesicles as conveyors of immune responses. Nat Rev Immunol 9: 581-593, 2009.
38. Yonemura Y, Endo Y, Yamaguchi T, Fujimura T, Obata T, Kawamura T, Nojima N, Miyazaki I and Sasaki T: Mechanisms of the formation of the peritoneal dissemination in gastric cancer. Int J Oncol 8: 795-802, 1996.
39. Nishimori H, Yasoshima T, Denno R, Shishido T, Hata F, Okada Y, Ura H, Yamaguchi K, Isomura H, Sato N, *et al*: A novel experimental mouse model of peritoneal dissemination of human gastric cancer cells: Different mechanisms in peritoneal dissemination and hematogenous metastasis. Jpn J Cancer Res 91: 715-722, 2000.
40. López-Terrada D, Cheung SW, Finegold MJ and Knowles BB: Hep G2 is a hepatoblastoma-derived cell line. Hum Pathol 40: 1512-1515, 2009.